International Journal of Nanoelectronics and Materials
IJNeaM
ISSN 1985-5761 | E-ISSN 2232-1535

Turning waste into strength: Enhancing geopolymer composites with Oil Palm Frond Fibers (OPF)

Ng Hui-Teng [a], Liew Yun-Ming [a,b] *, Heah Cheng-Yong [a,c], Tan Soo Jin [c], Tan You How [d], Muhammad Aqil Asyraf Bin Mohd Roslan [b], Siti Khadijah Binti Zulkepli [b], Ng Yong-Sing [e]

[a]*Geopolymer and Green Technology, Centre of Excellence (CEGeoGTech), Universiti Malaysia Perlis (UniMAP), 01000 Perlis, Malaysia*
[b]*Faculty of Chemical Engineering Technology, Universiti Malaysia Perlis (UniMAP), 01000 Perlis, Malaysia*
[c]*Faculty of Mechanical Engineering Technology, Universiti Malaysia Perlis (UniMAP), 02600 Perlis, Malaysia*
[d]*Grenoh Solution, No. 1, Taman Cempaka Jementah, 85200 Segamat, Johor*
[e]*Centre for Advanced Materials, Department of Manufacturing Technology, Faculty of Engineering and Technology, Tunku Abdul Rahman University of Management and Technology, 53300, Kuala Lumpur, Malaysia*
** Corresponding author. Tel.: +60174968530; e-mail: ymliew@unimap.edu.my*

Received 18 January 2024, Revised 2 April 2024, Accepted 17 April 2024

ABSTRACT

Geopolymers are alternatives to ordinary Portland cement as construction materials. The increasing demand for sustainable construction materials has driven the utilization of industrial by-products and agricultural waste. The disposal of oil palm frond (OPF) biomass as waste in landfills poses significant environmental challenges, necessitating effective recycling strategies. This study examines the incorporation and feasibility of OPF as a reinforcing fiber in fly ash geopolymer composites, examining its impact on physical and mechanical properties. Various parameters were tested, including fiber content (10–20 wt.%), shapes (shredded and tubular), and lengths (1–3 cm). The geopolymer composites with 10 wt.% shredded oil palm frond and 1-cm tubular oil palm frond fibers enhance the compressive strength by 17% compared to the control sample without oil palm frond. The shredded oil palm frond was particularly effective, enhancing strength performance and achieving better dispersion within the geopolymer matrix. Conversely, increasing the fiber content and length generally resulted in diminished composite strength, attributed to the creation of a more porous structure and weaker fiber-matrix interactions. However, lower fiber additions were shown to decrease porosity and water absorption, highlighting the potential of optimized oil palm frond fiber content and form in improving the environmental and mechanical performance of geopolymer composites. These results support the viability of oil palm frond as a sustainable additive in geopolymers, contributing to waste reduction and material innovation in construction.

Keywords: *Geopolymer, Composites, Natural Fiber, Oil Palm Frond*

1. INTRODUCTION

Geopolymer technology is experiencing rapid advancements due to its superior properties, including remarkable physico-mechanical and thermal properties, resistance to chemical and fire, sustainability, durability, and environmentally friendly benefits such as energy conservation, reduced carbon emissions, and effective waste utilization [1]. Industrial by-products like fly ash are repurposed to produce geopolymers through an alkali-activation process using sodium or potassium solutions. This process allows fly ash to contribute silicon and aluminum, while the alkali solutions provide silicon and sodium for geopolymerization.

Despite the impressive performance of geopolymers, continuous research efforts aim to enhance their performance further. One innovative approach has been the introduction of natural fibers, including coir, coconut, cotton, raffia, straw, and sisal, into geopolymer composites [2]. Particularly, fibers from oil palm trunks (OPT) and oil palm fronds (OPF) have been explored, with OPT already being incorporated into geopolymer products [3] and OPF being used in more limited applications such as bricks [4] and panels [5]. Given this, it becomes crucial to explore the potential of OPF fibers in geopolymer applications more extensively.

OPF represents a significant portion of biomass waste from oil palm cultivation, alongside other materials like OPT, oil palm shell, clinker, leaves, and fuel ash [3]. In Malaysia, the world's second-largest exporter of palm oil after Indonesia, the oil palm industry generates a substantial amount of biomass waste, with OPF accounting for approximately 70% of this total. Annually, Malaysia produces around 12.9 million tons of OPF [6]. The majority of this biomass waste ends up in landfills, posing environmental risks. There is a pressing need to recycle this abundant waste stream into high-value products, particularly geopolymer composites.

This study proposes the reinforcement of OPF into geopolymers to create novel geopolymer composites. The abundance of OPF, coupled with its underutilization in existing geopolymer formulations, underscores the

potential for innovative applications. The study investigates various OPF integration parameters, including shapes (shredded and tubular), contents (10, 15, and 20 wt.%), and length of tubular fibers (1, 2, and 3 cm). Key performance indicators such as bulk density, water absorption, apparent porosity, compressive strength, and microstructural properties were examined to understand the impact of these parameters on the resulting geopolymer composites. The exploration of OPF in geopolymers not only addresses environmental issues but also pushes the boundaries of material science by developing new, sustainable construction materials.

2. METHODOLOGY

2.1. Materials

Class F fly ash (Manjung Electric Power Plants, Perak, Malaysia) was used as the aluminosilicate material. Table 1 tabulates the chemical composition of fly ash determined using X-ray fluorescence (XRF). The fly ash contains 37% of SiO_2, 20% of Al_2O_3 and 12% of CaO. The fly ash particles are spherical with smooth surfaces (Figure 1).

Alkali activator was prepared using sodium silicate (South Pacific Chemical Industry Sdn. Bhd., Malaysia) and 10M sodium hydroxide (Progressive Scientific Sdn. Bhd., Malaysia) solution at a ratio of 2.5. The sodium silicate comprises 60.5 wt.% of H_2O, 30.1 wt.% SiO_2 and 9.4 wt.% of Na_2O. The sodium hydroxide has a purity of 99% in the form of a pellet.

OPF in shredded and tubular shapes (Figure 2) were incorporated in geopolymer paste to produce geopolymer composites. The as-received shredded OPF was used without any treatment while the tubular OPF was cut into lengths of 1 cm, 2 cm and 3 cm. The OPF was added into the geopolymer paste at 10 wt.%, 15 wt.% and 20 wt.% calculated upon the weight of fly ash (180 g).

2.2. Preparation of Geopolymer Composites

Alkali activator was added to the fly ash at a fly ash/alkali activator ratio of 2.0 and stirred for 2 minutes to obtain a homogeneous slurry. The OPF was then added to the geopolymer paste and stirred for another 2 minutes. The geopolymer composite was cast into a 50 mm × 50 mm × 50 mm mould and compacted to remove entrapped air. The fresh geopolymer composite was cured at room temperature for 24 hours. The hardened geopolymer composite was then removed from the mould and wrapped with a thin film to hinder moisture loss. The hardened geopolymer composite was aged for 27 days at room temperature prior to testing.

Table 1. Chemical composition of fly ash

Oxide	Weight percentage (wt. %)
Na_2O	3.41
MgO	4.95
Al_2O_3	20.67
SiO_2	36.97
P_2O_5	1.04
SO_3	1.80
K_2O	1.62
CaO	12.47
Sc_2O_3	1.79
Fe_2O_3	13.00
Other	2.29

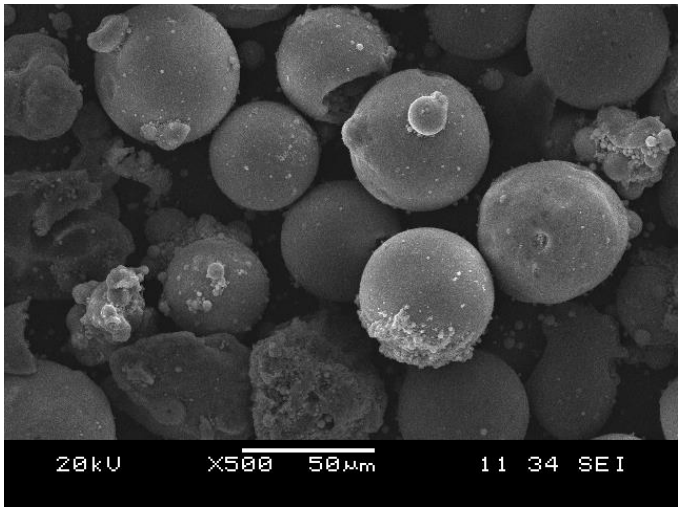

Figure 1. Microstructure of fly ash

Figure 2. Images of (a) shredded and (b) tubular OPF

2.3. Test and Characterization

The bulk density measurement was performed based on BS EN 12390-7 by measuring the mass and volume of the geopolymer composites. A vernier caliper was used to measure the sample's dimensions, whereas an electronic balance was used to measure the mass.

The water absorption and apparent porosity of the geopolymer were tested in accordance with ASTM C2000. The dry mass (M_d) was measured after drying at 85°C for 24 hours. The sample was then immersed in water for 24 hours and its weight was measured as wet mass (M_w). The weight of the sample suspended in water was measured as suspended mass (M_s). The water absorption and apparent porosity were calculated using Equations (1) and (2).

$$\text{Water Absorption} = (M_w - M_d)/M_d \times 100\% \quad (1)$$

$$\text{Apparent Porosity} = (M_w - M_d)/(M_w - M_s) \times 100\% \quad (2)$$

The compressive test was performed on the geopolymer composite based on ASTM C109 using a Shimadzu UH-100 kN universal testing machine with a constant loading rate of 5 mm/min. Three geopolymer composites were tested to obtain the average compressive strength value.

The microstructure of fly ash and geopolymer composite was examined using the JSM-6460 LA scanning electron microscope (SEM) with an accelerating voltage of 10 kV and a working distance of 10 mm. The fly ash was in powder form while the geopolymer composite was a fragment of sample. The specimen for analysis was coated with palladium using an Auto Fine Coater to prevent electrostatic charge during imaging. The elemental composition of the geopolymer composite was analyzed with Energy Dispersive X-ray Spectroscopy (EDS).

The phase analysis of fly ash and geopolymer composite was performed using a Bucker D2 Phaser X-Ray Diffractor (XRD), scanning from 10° to 80° 2θ with a constant rate of 2°/min and a scan step of 0.02° with radiation of Cu-Kα at 40 kV and 35 mA. The specimen for analysis was ground powder.

The structural analysis of fly ash and geopolymer composite was analysed using Perkin Elmer Fourier Transform Infrared (FTIR) Spectroscopy, scanning from 650 cm^{-1} to 4000 cm^{-1} with a constant resolution of 4 cm^{-1}. The specimen for analysis was ground powder.

3. RESULTS AND DISCUSSION

3.1. Physical Properties

The fly ash geopolymers exhibited a bulk density of 1.84 g/cm^3, apparent porosity of 12.1% and water absorption of 11.9% (Figure 3). Adding OPF in the geopolymer matrix reduced the bulk density in general, as plant fibers are lignocellulosic [7], which contributed to additional pores inthe geopolymer matrix. In contrast, the apparent porosity and water absorption were reduced after adding low content of OPF (10 wt.%). This was more obvious when adding shredded OPF as it would fill the gap between the geopolymer matrix, producing a compact matrix.

The bulk densities of geopolymer composites declined with increasing OPF contents, regardless of the shape of OPF added (Figure 3a). The result was accompanied by an increase in water absorption (Figure 3b) and apparent porosity (Figure 3c). By adding shredded OPF, a higher bulk density (1.5–1.9 g/cm^3) was recorded with lower water absorption (4.2–7.7%) and apparent porosity (8.6–15.4%). On the other hand, geopolymer composites added with tubular OPF had comparatively lower bulk density (1.4–1.8 g/cm^3) and higher water absorption (6.9–12.9%) and apparent porosity (13.5–27.4%).

As mentioned above, plant fibers are lignocellulose which is light in weight and highly porous. They are also strongly polar and hydrophilic [8]. Thus, the greater amount of OPF incorporated in the geopolymer matrix caused the inclusion of more porous and lightweight OPF [9], which decreased the bulk density. The highly porous OPF tended to absorb more water, contributing to higher water absorption values. When the OPF was added in shredded form, the geopolymer slurry tended to wet the plant fiber which led to generally lower porosity, but a higher bulk density and water absorption compared to that incorporated with tubular OPF. Similarly, when longer tubular OPF with increasing length was used, the hollow portion of tubular OPF increased, increasing the porosity and water absorption while decreasing the bulk density. The result was also supported by Ribeiro *et al.* [8] who reported the reduced penetration of water in the geopolymer composites due to fiber addition. Despite the addition of fiber restricting the penetration of water, it contributed to higher water absorption of geopolymer composites due to the hydrophilic character, as aforementioned. However, the water absorption reported in the present study was lower than that reported by Ribeiro *et al.* [8] who recorded water absorption up to 36.5% for metakaolin geopolymer reinforced with alkali-treated bamboo fiber.

3.2. Compressive Strength

Figure 4 presents the compressive strength of FA geopolymer and geopolymer composites added with shredded and tubular OPF. The FA geopolymer possessed a compressive strength of 26.4 MPa after 28 days. The addition of small amounts of OPF, particularly 10 wt.% of shredded and 10-mm tubular OPF, enhanced the compressive strength of the geopolymer composites. A comparative compressive strength (~31 MPa) was achieved with 10 wt.% of shredded and tubular OPF (10 mm length). Based on Abbas *et al.* [10], fibers act as bridges across the microcracks induced by stress, stopping the propagation of cracks within the geopolymer matrix. Good fiber-matrix interaction enhances energy absorption, improving the mechanical strength of geopolymer composites [11].

However, Increasing OPF content degraded compressive strength, regardless of the shapes of OPF. In general, the

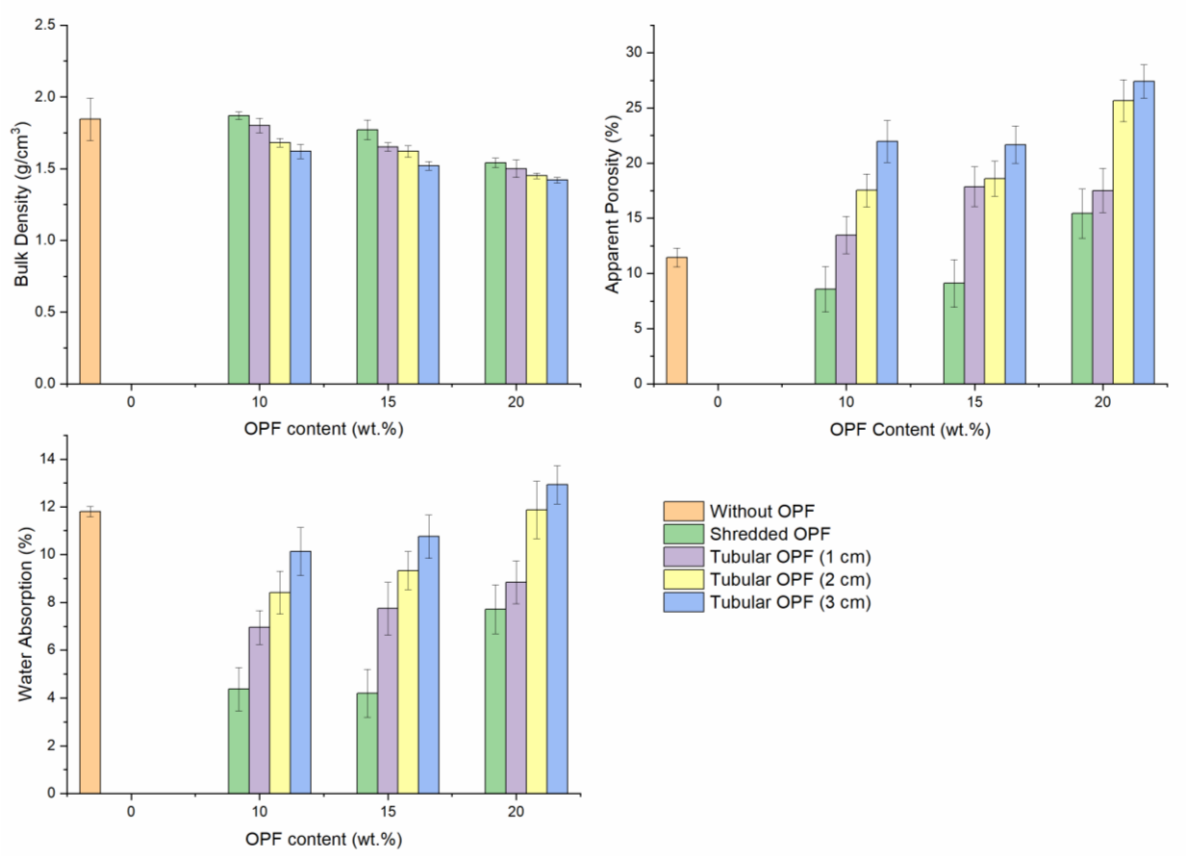

Figure 3. (a) Bulk density; (b) water absorption; and (c) apparent porosity of geopolymer composites added with shredded and tubular OPF

compressive strength recorded for geopolymer composite with tubular OPF (6.4–30.9 MPa) was lower than that with shredded OPF (9.9–31.7 MPa). This was due to the higher porosity induced by tubular OPF compared to shredded OPF (Figure 3). The tubular OPF hindered the matrix connectivity and weakened the internal structure. The shredded OPF had a better bridging effect with the geopolymer matrix. Aggregation due to excessive OPF occurred, resulting in a poor workable mixture and subsequently loose interior structure. The compressive strength trend aligned with the bulk density, water absorption and porosity as shown in Figure 3.

Increasing the length of tubular OPF tended to reduce the compressive strength by 32.5–37.1% due to increased pores within the geopolymer matrix and the poor adhesion between OPF and the geopolymer matrix as stated above. This was supported by the increasing pores with increased in the tubular OPF and contributed to increased overall porosity of the geopolymer sample as illustrated in Figures 3c and 5. During the mixing in the geopolymer matrix, it is difficult to make sure the OPF will distribute uniformly. As consequences, the tubular OPF collided with each other forming more pores and cavities. The reduction of compressive strength with increasing length was consistent with the observation reported by Ribeiro *et al.* [12] for geopolymer composites added with alkali-treated micro bamboo fibers.

As compared to the natural fiber-incorporated geopolymer composites produced by Ye *et al.* [13], the compressive strength of geopolymer composites prepared in this study (20–31 MPa) outperformed those added with lignin, cellulose and hemicellulose in metakaolin geopolymer (9–10 MPa), with the same fiber content (10 wt.%). However, when the fiber content increased to 20 wt.%, the compressive strength increased for the metakaolin geopolymer composites produced by Ye *et al.* [13], particularly for those added with lignin. An increase in hemicellulose would reduce the degree of geopolymerization. The comparison of the compressive strength of geopolymer composites added with different fibers is presented in Figure 6.

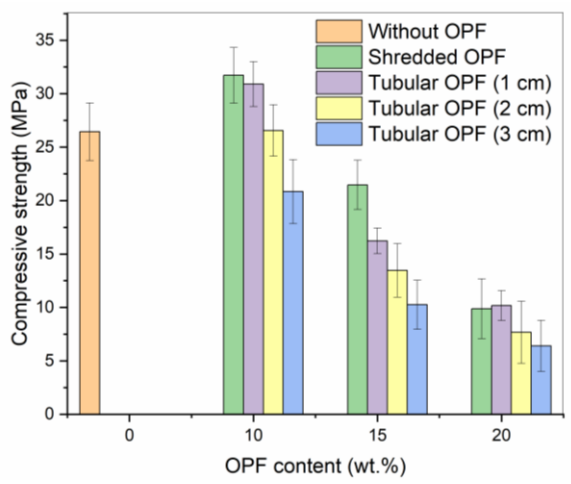

Figure 4. Compressive strength after 28 days of geopolymer composites added with shredded and tubular OPF

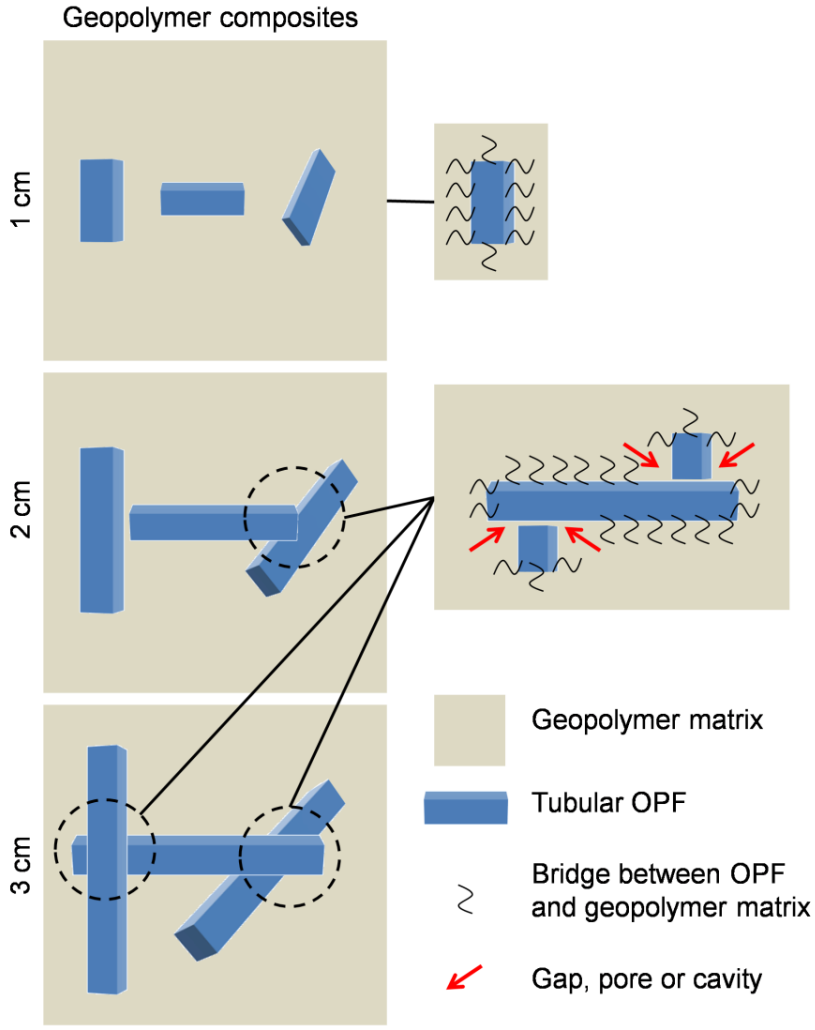

Figure 5. Schematic diagram of geopolymer composites with varying tubular OPF lengths

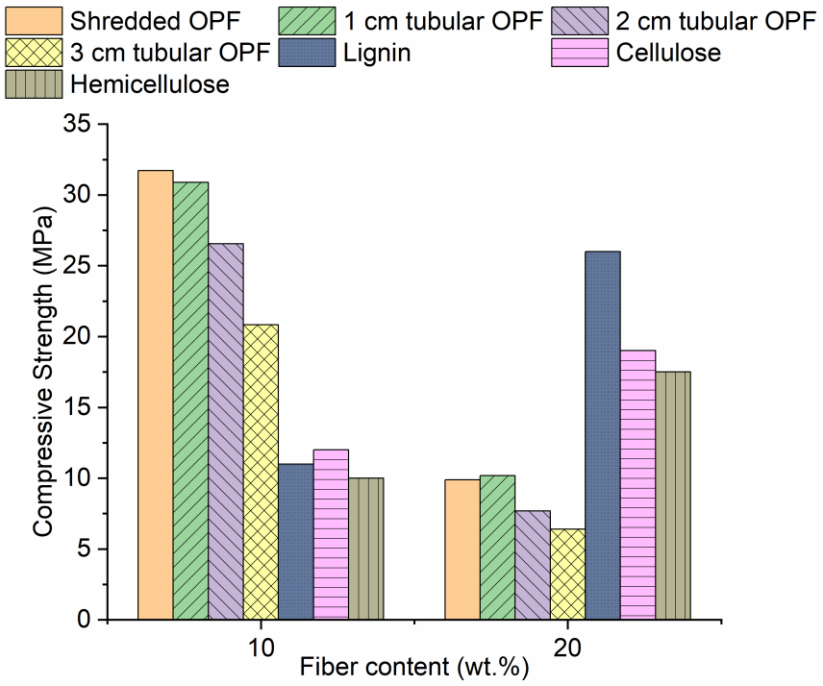

Figure 6. Comparison of the compressive strength of geopolymer composites added with varying fibers [13]

3.3. Microstructural Analysis

Figure 7 reveals the fracture surfaces of geopolymer composites without the addition of shredded and tubular OPF. The microstructure of geopolymer composites was heterogeneous, comprising pores, unreacted FA [as shown by spherical particles (Figure 1)] and OPF. At a low fiber content of 10 wt.%, the OPF had a better dispersion and bridging with the geopolymer matrix (Figures 8a and 8b). In comparison, the shredded OPF distributed more homogeneously than tubular OPF in the geopolymer matrix. With increasing fiber content, aggregation of shredded OPF became more obvious as evidenced by the agglomeration of the larger portion of OPF, causing weaker interaction with the geopolymer matrix (Figures 8c and 8d). Increasing the fiber content would severely impact the workability of the geopolymer matrix and affect the packing of the fiber in the geopolymer matrix [10].

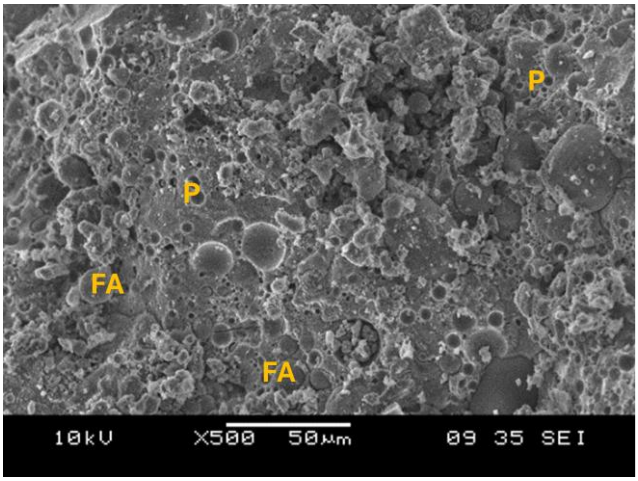

Figure 7. SEM micrograph of control fly ash geopolymer without addition of OPF (FA – unreacted fly ash and P – pores)

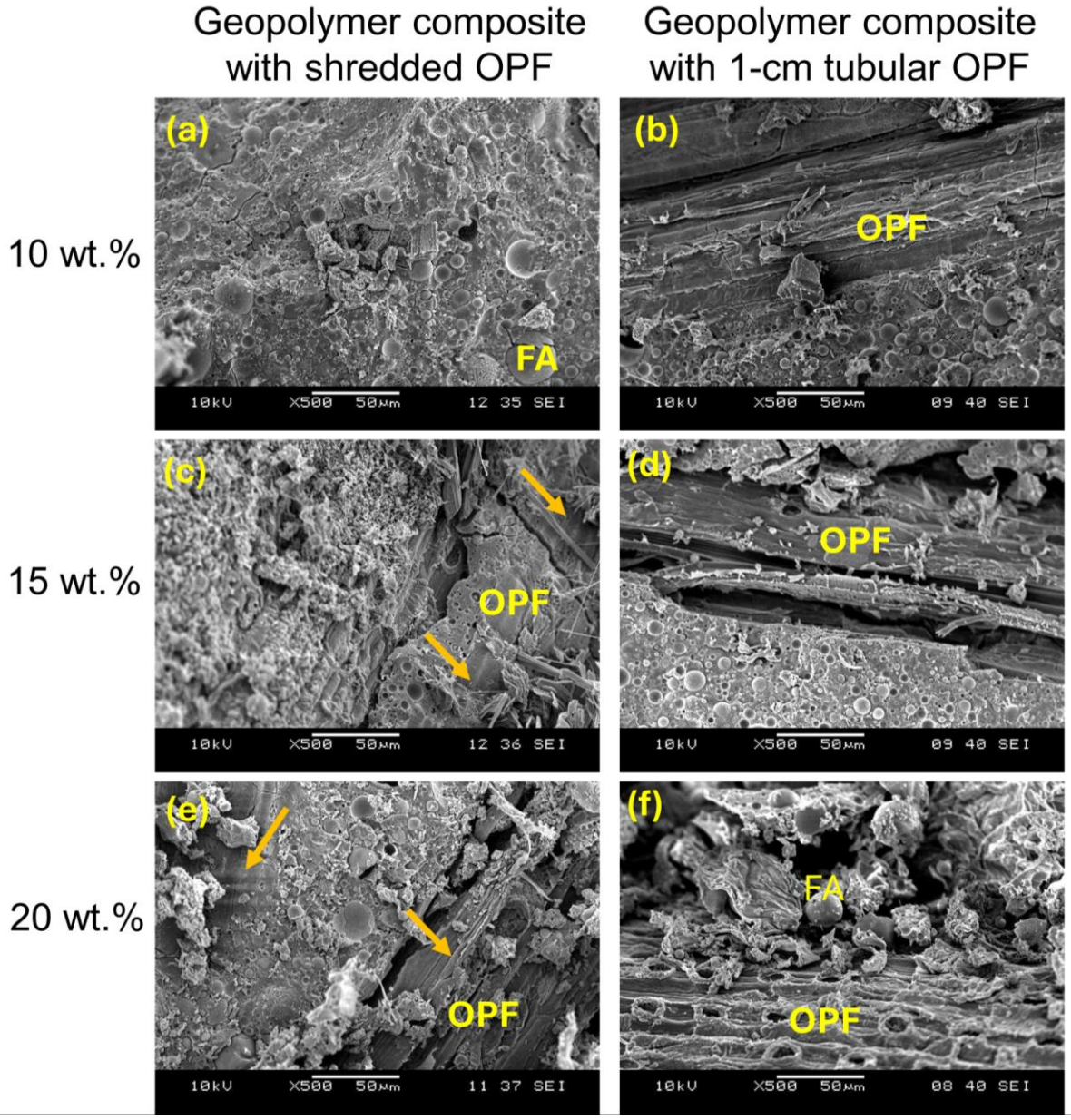

Figure 8. SEM micrographs of geopolymer composites added with shredded OPF (a, c, e) and 1 cm tubular OPF (b, d, f) with different fiber contents (FA is fly ash, GM is geopolymer matrix and arrow represents the agglomeration of shredded OPF)

Similarly, the bonding between tubular OPF and geopolymer matrix was weak with pores and gaps with increasing fiber content, especially obvious in geopolymer composites with 20 wt.% of tubular OPF (Figure 8f). The increasing fiber content, in conjunction with the absorbing capability of fiber materials, also caused difficulty in packing fiber and geopolymer materials and insufficient alkali activator for the geopolymerization reaction to form the dense matrix. The voids acted as the stress concentration points when force was applied. This observation ascertained the decreasing compressive strength of geopolymer composites with increasing shredded OPF and tubular OPF (Figure 4). Ranjbar *et al.* [14] further confirmed that the poor compaction of fiber content in composites during the fresh state leads to an extremely porous structure and heterogeneous fiber-matrix interaction. The interface and adhesion between the natural fiber and the geopolymer matrix play an important role in determining the physical and mechanical properties of the geopolymer composites [8].

3.4. Phase and Functional Group Analyses

Figure 9 illustrates the XRD diffractogram and FTIR spectra of fly ash and geopolymer. The analysis was done on the geopolymer paste. The OPF did not take part in the geopolymerization reaction. This was supported by Ranjbar *et al.* [15] who prepared fiber-reinforced geopolymer concrete, implying the insignificant effect of fiber on the geopolymerization reaction.

Fly ash showed primary diffraction peaks of mullite (ICDD# 00-006-0259) and quartz (ICDD# 01-078-1259) with diffuse halo at 2θ of 15°–35° (Figure 9a). After alkali activation, the diffuse halo shifted to a higher degree in the range of 20°–40° 2θ. The shift implied the formation of a geopolymer matrix [16].

On the other hand, the FTIR spectrum of fly ash (Figure 9b) contained mainly Si-O-Al and Si-O-Si asymmetric stretching vibrations at 1031 cm^{-1} [17]. The formation of geopolymer networks shifted the absorption band to a lower wavenumber of 983 cm^{-1}. It was corresponding to the sodium aluminate silicate hydrate (N-A-S-H) gel [18]. The bands at ~3400 cm^{-1}, 1651 cm^{-1} and 1415 cm^{-1} were separately assigned as OH and H-O-H stretching vibration [19], H-O-H bending vibration [20] and O-C-O stretching vibration [21].

4. CONCLUSION

This paper investigates the physical and mechanical properties of fly ash geopolymer composites added with various fiber contents (10–20 wt.%), shapes (shredded and tubular) and lengths (1–3 cm). The fly ash geopolymer composites with 10 wt.% of shredded OPF and 10-mm tubular OPF showed improvement of compressive strength (~31.0 MPa) by 17% compared to the fly ash geopolymer without the addition of OPF (26.4 MPa). The shredded shapes of OPF led to better strength performance and dispersion of fiber in the geopolymer matrix compared to tubular OPF. Increasing fiber content and length was not beneficial for strengthening of geopolymer matrix due to the porous structure and weak fiber-matrix interface. Adding low shredded OPF (<15 wt.%) in the geopolymer matrix reduced the porosity and water absorption. The findings of the work showed that geopolymer composites incorporated with OPF can be potentially used as sustainable building materials.

ACKNOWLEDGMENTS

The authors express gratitude to UniMAP-Private Matching Fund (UniPRIMA) (9002-00148 and 9001-00709) for their financial support. Additionally, appreciation is extended to Grenoh Solution and Sultan Azlan Shah Power Station, TNB Janamanjung, Malaysia for providing the oil palm frond and fly ash utilized in this study.

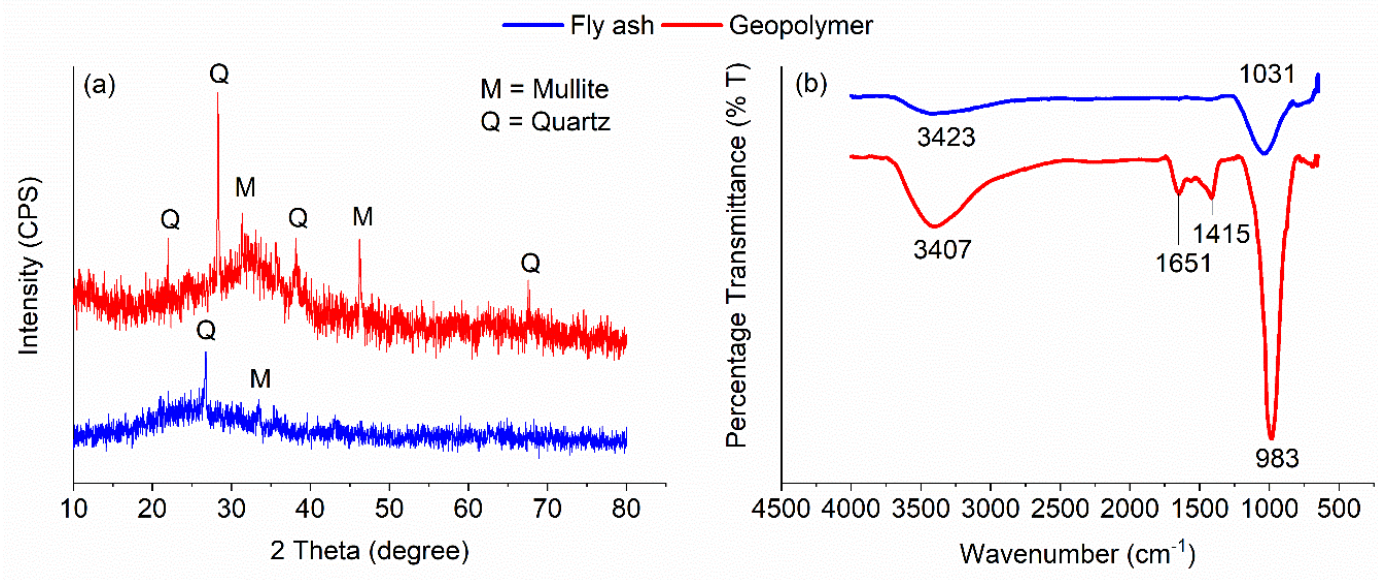

Figure 9. (a) XRD diffractogram and (b) FTIR spectra of fly ash and geopolymer

REFERENCES

[1] M. Amran, S. Debbarma, and T. Ozbakkaloglu, "Fly ash-based eco-friendly geopolymer concrete: A critical review of the long-term durability properties," *Construction and Building Materials*, vol. 270, p. 121857, 2021.

[2] G. Silva, S. Kim, R. Aguilar, and J. Nakamatsu, "Natural fibers as reinforcement additives for geopolymers – A review of potential eco-friendly applications to the construction industry," *Sustainable Materials and Technologies*, vol. 23, p. e00132, 2020.

[3] A. B. Malkawi, M. Habib, J. Aladwan, and Y. Alzubi, "Engineering properties of fibre reinforced lightweight geopolymer concrete using palm oil biowastes," *Australian Journal of Civil Engineering*, vol. 18, no. 1, pp. 82–92, 2020.

[4] J. B. Niyomukiza, K. C. Nabitaka, M. Kiwanuka, P. Tiboti, and J. Akampulira, "Enhancing Properties of Unfired Clay Bricks Using Palm Fronds and Palm Seeds," *Results in Engineering*, vol. 16, p. 100632, 2022.

[5] I. Khalid, O. Sulaiman, R. Hashim, W. Razak, N. Jumhuri, and M. S. M. Rasat, "Evaluation on layering effects and adhesive rates of laminated compressed composite panels made from oil palm (Elaeis guineensis) fronds," *Materials & Design*, vol. 68, pp. 24–28, 2015.

[6] H. M. Hamada *et al.*, "The use of palm oil clinker as a sustainable construction material: A review," *Cement and Concrete Composites*, vol. 106, p. 103447, 2020.

[7] H. A. Santana, N. S. Amorim Júnior, D. V. Ribeiro, M. S. Cilla, and C. M. R. Dias, "Vegetable fibers behavior in geopolymers and alkali-activated cement based matrices: A review," *Journal of Building Engineering*, vol. 44, p. 103291, 2021.

[8] M. G. Sá Ribeiro, I. P. A. Miranda, W. M. Kriven, A. Ozer, and R. A. Sá Ribeiro, "High strength and low water absorption of bamboo fiber-reinforced geopolymer composites," *Construction and Building Materials*, vol. 411, p. 134179, 2024.

[9] Z. X. Ooi, Y. P. Teoh, B. Kunasundari, and S. H. Shuit, "Oil palm frond as a sustainable and promising biomass source in Malaysia: A review," *Environmental Progress & Sustainable Energy*, vol. 36, no. 6, pp. 1864–1874, 2017.

[10] A.-G. N. Abbas, F. N. A. A. Aziz, K. Abdan, N. A. M. Nasir, and G. F. Huseien, "A state-of-the-art review on fibre-reinforced geopolymer composites," *Construction and Building Materials*, vol. 330, p. 127187, 2022.

[11] G. Silva, S. Kim, B. Bertolotti, J. Nakamatsu, and R. Aguilar, "Optimization of a reinforced geopolymer composite using natural fibers and construction wastes," *Construction and Building Materials*, vol. 258, p. 119697, 2020.

[12] M. G. Sá Ribeiro, M. G. Sá Ribeiro, P. F. Keane, M. R. Sardela, W. M. Kriven, and R. A. Sá Ribeiro, "Acid resistance of metakaolin-based, bamboo fiber geopolymer composites," *Construction and Building Materials*, vol. 302, p. 124194, 2021.

[13] H. Ye, Y. Zhang, Z. Yu, and J. Mu, "Effects of cellulose, hemicellulose, and lignin on the morphology and mechanical properties of metakaolin-based geopolymer," *Construction and Building Materials*, vol. 173, pp. 10–16, 2018.

[14] N. Ranjbar and M. Zhang, "Fiber-reinforced geopolymer composites: A review," *Cement and Concrete Composites*, vol. 107, p. 103498, 2020.

[15] N. Ranjbar, M. Mehrali, M. Mehrali, U. J. Alengaram, and M. Z. Jumaat, "High tensile strength fly ash based geopolymer composite using copper coated micro steel fiber," *Construction and Building Materials*, vol. 112, pp. 629–638, 2016.

[16] N. Yong-Sing *et al.*, "Evaluation of flexural properties and characterisation of 10-mm thin geopolymer based on fly ash and ladle furnace slag," *Journal of Materials Research and Technology*, vol. 15, pp. 163–176, 2021.

[17] Y. Liu, W. Zhu, and E.-H. Yang, "Alkali-activated ground granulated blast-furnace slag incorporating incinerator fly ash as a potential binder," *Construction and Building Materials*, vol. 112, pp. 1005–1012, 2016.

[18] N. Hui-Teng *et al.*, "Thermo-mechanical behaviour of fly ash-ladle furnace slag blended geopolymer with incorporation of decahydrate borax," *Construction and Building Materials*, vol. 331, p. 127337, 2022.

[19] J. K. Prusty and B. Pradhan, "Multi-response optimization using Taguchi-Grey relational analysis for composition of fly ash-ground granulated blast furnace slag based geopolymer concrete," *Construction and Building Materials*, vol. 241, p. 118049, 2020.

[20] I. G, B. Singh, S. Deshwal, and S. K. Bhattacharyya, "Effect of sodium carbonate/sodium silicate activator on the rheology, geopolymerization and strength of fly ash/slag geopolymer pastes," *Cement and Concrete Composites*, vol. 97, pp. 226–238, 2019.

[21] A. Bouaissi, L. Li, M. M. Al Bakri Abdullah, and Q.-B. Bui, "Mechanical properties and microstructure analysis of FA-GGBS-HMNS based geopolymer concrete," *Construction and Building Materials*, vol. 210, pp. 198–209, 2019.